Journal of Stress Analysis
Vol. 4, No. 2, Autumn – Winter 2019-20
Bu-Ali Sina University

Investigation of Residual Stress in the Ultrasonic Assisted Constraint Groove Pressing Process of Copper Sheets

M. Asgari, M. Honarpisheh*, S. Amini, H. Mansouri
Faculty of Mechanical Engineering, University of Kashan, Kashan, Iran.

Article info

Article history:
Received 10 December 2019
Received in revised form
31 January 2020
Accepted 11 March 2020

Keywords:
Constraint groove pressing
Ultrasonic vibrations
Residual stress
Contour method

Abstract

In this research, Constraint Groove Pressing (CGP) process, which is one of the most important and effective methods of severe plastic deformation processes has been studied. Ultrasonic assisted CGP (UCGP) process has been conducted to investigate and compare the effects of applying ultrasonic vibrations on the residual stress with the conventional method. Contour method was applied to measure the residual stresses distributions in the CGPed and UCGPed samples. Pure copper sheet samples were tested both with and without ultrasonic vibrations up to 2 passes. The measured values of the residual stresses indicated a relative reduction of stress in the presence of ultrasonic vibrations. By investigation of residual stress normal to the surface in thickness direction, it was observed that residual stresses are compressive on the edge and tensile in the middle of the thickness of the sheet. This reflects the self-balancing feature of residual stresses. In all conditions for both passes, residual stress reduced about 20MPa while using ultrasonic vibrations compared to traditional CGP method.

1. Introduction

Constrained Groove Pressing (CGP) is one of the Severe Plastic Deformation (SPD) processes. In this method, the strain is applied in a constrained condition to a sheet, and thus the bending strain or non-uniformity of the strain does not occur significantly. As the mechanical analysis demonstrated, in this method, the deformation is applied under the plane strain conditions with pure shear. Shin et al. proposed the CGP method for the first time [1]. A schematic of this method is shown in Fig. 1.

In this method, a metal plate is placed between two molds with an asymmetric groove and is pressed. In this case, the inclined parts of the sheet are deformed in plane strain condition under shear stresses, while no strain is applied to the flat parts of the sheet (unhatched areas). When the angle of the inclined part is 45 degrees (θ angle), the shear strain rate of the action is equal to one, resulting in an effective strain of about 0.58 to the inclined parts [2]. In the second step, the sheet is pressed between two flat sheets and returns to its original dimensions. At this stage, the deformed regions in the first stage are once more subjected to shear deformation and the strain rate is doubled in these areas, while no strain is applied to the undeformed regions. The metal plate then revolves 180 degrees around the axis, perpendicular to the surface of the sheet, and the steps of the CGP are once more repeated with grooved and flat molds so that at this stage, the un-deformed regions in two previous presses are subjected to shear strains, and thus the strain distribution in the metal plate becomes more uniform. By following these steps, high strains are stored in sheet, resulting into a nano or ultrafine grained structure [1, 3-5].

*Corresponding author: M. Honarpisheh (Associate Professor)
E-mail address: honarpishe@kashanu.ac.ir
http://dx.doi.org/10.22084/jrstan.2020.20568.1119
ISSN: 2588-2597

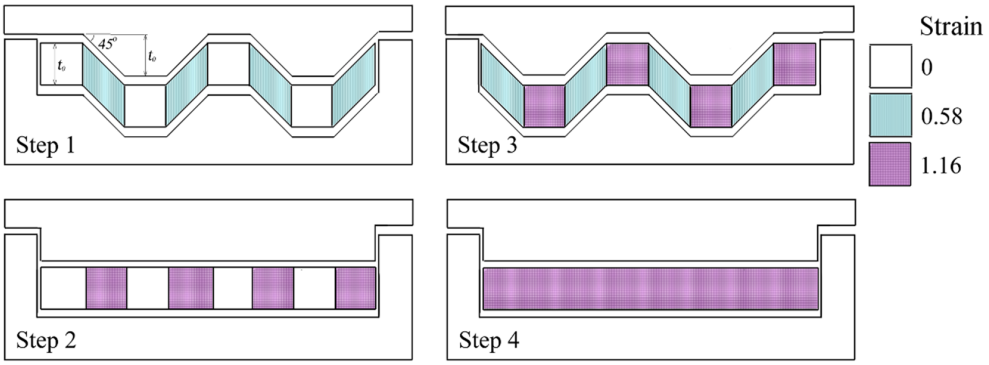

Fig. 1. The schematic steps of CGP process.

If the CGP operation is considered to be a type of forming operation, the groove depth for pure commercial aluminum samples should not exceed 2.5 times more than the thickness of the sheet [3, 6, 7]. In the CGP process, th friction between the mold and the sample causes the formation of micro cracks during pressing. The surface cracks develop in the higher passes and eventually cause the sample failure. It's possible to apply higher strains in the CGP process. To this end, as the friction between the contact surfaces reduces as a result of decreases in the surface cracks, it is possible to apply higher strain. The effect of friction reduction between the mold and the sample surfaces has recently been reported by Hosseini et al. In this study, Teflon layers were used as lubricants to reduce friction, which contributed to the possibility of applying 7 passes of CGP to pure aluminum specimens [8, 9], while, in previous studies, at most 4 passes could be applied to aluminum samples without using a lubricant [9-11].

Thus far, the CGP process has been applied to various metals such as aluminum, steel, titanium, copper, magnesium, and there are quite a few papers on the obtained results [1, 9, 10, 12-17]. Nazari and Honarpisheh modeled CGP analytically to estimate forces and to examine the behavior of the sheet. The findings showed that Von-Mises is more suitable yield criterion than Tresca for CGP force estimation [18], and, in the same year, they investigated the effect of deformation behavior and effective strain on the CGPed sheet and reported that the pressing section has a significant effect on the properties of constrained groove pressed sheets [19]. One year after, in another study, they examined the effect of stress relief annealing on the residual stress of a copper sheet in the CGP process. Their result indicated that, the residual stress decreases by increasing the number of CGP passes. The results also showed that stress relief annealing increases residual stress due to increases in microstructure un-uniformity [20]. In SPD methods, the grain size is reduced to a nano-scale size and the mechanical properties of the metal improve significantly by applying severe strains to the sample.

Up to now, ultrasonic vibrations have been developed in processes such as tube drawing, wire drawing, deep drawing, extrusion, rolling, and upsetting [21].

Residual stresses are self-balancing stresses that are created in the work-piece due to the production process, such as rolling, welding, casting, machining, etc., which sometimes have negative and sometimes positive effects on the component life. Residual stresses can be beneficial or harmful due to their size and distribution related to external stress, which is harmful in most cases. Residual stresses also affect fatigue life. Residual stresses are measured in a variety of non-destructive, semi-destructive and destructive methods. There are some semi-destructive methods, such as hole drilling [22-24] and ring core [25, 26], destructive, like slitting [27-29], contour [30, 31] and inverse eigenstrain method [32] and non-destructive, like X-ray diffraction [33]. Destructive method of contour was used in this study to measure residual stress. The Contour method is one of the newest methods for measuring residual stresses, which was first introduced at a conference in 2000 [34]. In this method, the measurements of deformations caused by the release of stresses in the cutting process are used. The displacement data measured in the modeling and analysis of the finite element is used to calculate the residual stresses. It should be noted that the mean value of the data from both cut surfaces should be entered into the FEM software. As part of the analysis, displacements are measured as a set of boundary displacement conditions in the model. Contour measurement method is particularly suitable for complex residual stress fields with local variations, which are difficult to measure using conventional measurement methods. The area of uncertainty is usually around 0.5mm. However, through especial care near the edges, good results are obtained [35-39].

Alinaghian et al. investigated the influence of bending mode ultrasonic-assisted friction stir welding (BM-UAFSW) on longitudinal residual stress under various

vibration amplitudes of Al-6061-T6 alloy, and found that BMUAFSW process can decrease the maximum longitudinal residual stress up to 24% compared with the conventional FSW [40]. In another study, they investigated residual stresses after ultrasonic-assisted friction stir welding of AA 6061-T6. the findings indicated that high-frequency vibrations reduce the maximum tensile residual stress about 45% and, also, ultrasonic vibrations prevent defects such has voids and tunnel in weld zone due to peening effect in ultrasonic-assisted friction stir welding [41].

According to the author's knowledge and the findings of previous studies [18-20], the effects of ultrasonic vibrations in constraint groove pressing process has not been examined so far. In this paper, ultrasonic vibrations was applied to the copper sheets during the CGP process in order to examine the effects of ultrasonic vibrations on the residual stresses,.

2. Research Method

In this study, UCGP process, which is one of the SPD processes, was applied to pure commercial copper sheet to investigate the effect of utilizing ultrasonic vibrations on the residual stress of sheets compared to the conventional CGP process. Chemical composition of the sheet is shown in Table 1.

In this study, samples were prepared using the following conditions:

- Two samples (1 and 2 passes) were UCGPed to evaluate the residual stress.
- Two samples (1 and 2 passes) were CGPed to evaluate the residual stress.

After these treatments, the Contour method was used to measure the residual stresses. Fig. 2 shows the copper sample after the first pressing.

2.1. Tool Design

In this study, CK45 steel alloy was used as the tool material. This material has two good mechanical and acoustic features. The frequency used was 20KHz. Finite element software was used to determine the node points with C3D10 element type (Figs. 3a and 3b). After calculating and verifying the design using modal analysis in the ABAQUS finite element software, the horns were constructed and installed on the setup (Fig. 3c).

The resonant frequency obtained from the software for the groove and flat molding was 18616 and 18799Hz, respectively.

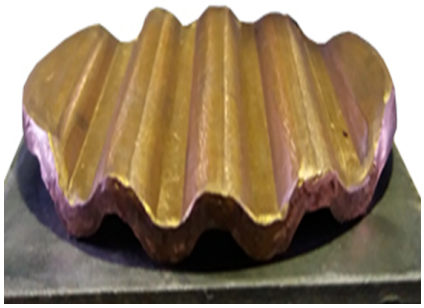

Fig. 2. Copper sample after the first grooving in the CGP process.

2.2. Residual Stress Measurement

After these treatments, the samples were compared with the Contour method for residual stress evaluation. The Contour method is almost unique in obtaining residual stresses in a two-dimensional cross section even in large parts. In this method, if it is possible, both surfaces should be measured at a given point, and it should be noted that when comparing two surfaces, one of the axes of the coordinates will be mirrored [35]. The data obtained from the measurement of both cutting surfaces should be balanced in a coordinate system and then averaged. In the finite element model, half of the original sample is designed. After performing the initial processing, the results have noises. These noises are corrected by manually removing and modifying information, averaging and smoothing the data curve, and also performing an experimental cut at the free end of the piece to examine the roughness of the cutting. Uncertainty in measuring strains near the edges should be considered as one of the disadvantages of the Contour method. The cutting width of the EDM may slightly change at the top and bottom of the cutting or at the beginning and the end of the cutting [42, 43]. As a result, data near the cutting edges cannot be completely reliable [35]. To measure the residual stresses, a copper sheet with 3mm thickness and 60mm diameter was prepared, annealed and CGPed up to 2 passes in two forms, with and without ultrasonic vibrations.

Table 1
Chemical composition of the pure commercial copper sheet.

Cu, %	Sn, %	Al, %	Pb, %	Ni, %	Fe, %
99.32	0.266	0.183	0.100	0.017	0.046
Si, %	Mn, ppm	As, ppm	P, ppm	Co, ppm	Sb, %
0.014	0.260	86.054	14.115	97.95	0.034

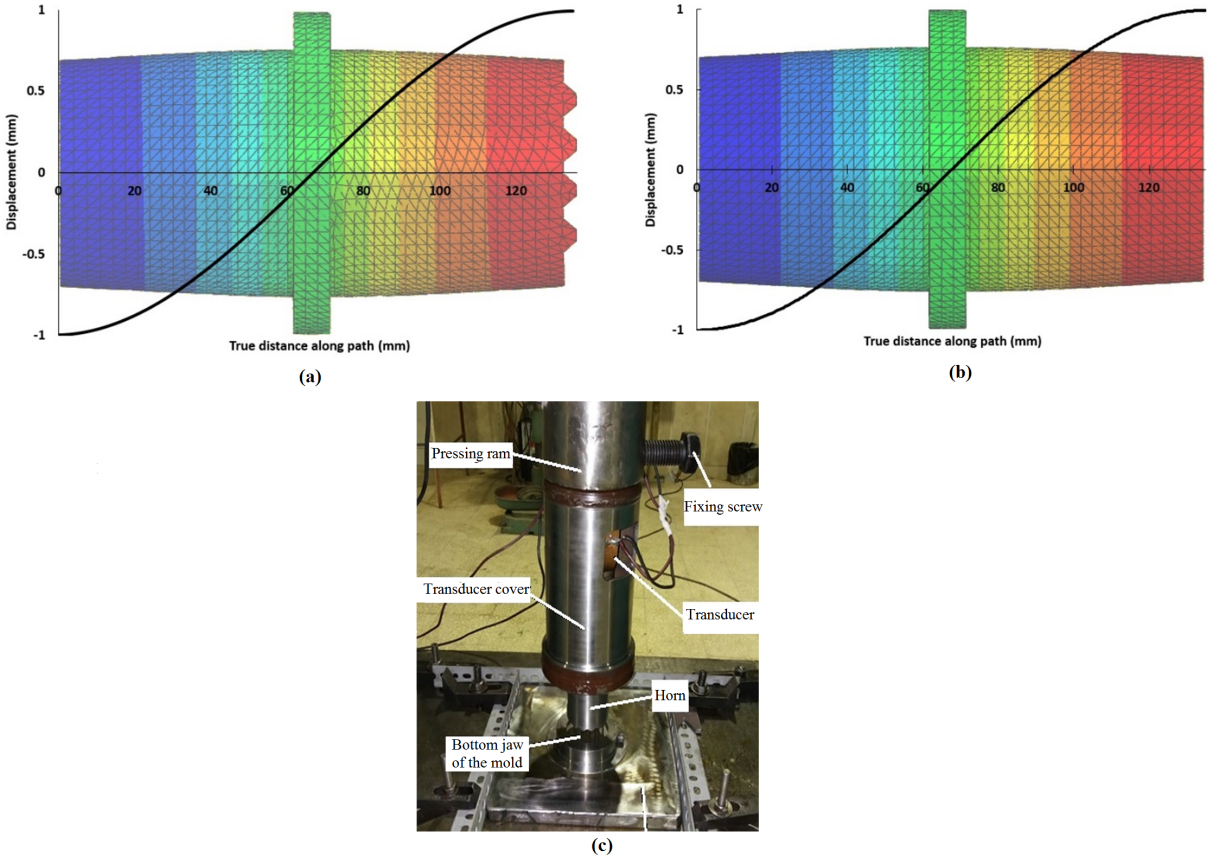

Fig. 3. Horn displacement curve along its length and the placement of the flange on the node location for a) Grooved horn, b) Flat horn, and c) Completed UCGP setup.

After performing the CGP process, the specimens were cut using the CHARMILLES ROBOFIL® Switzerland EDM machine, with 25 microns diameter brass wire, on finishing mode, and prepared to measure surface displacement. Samples were prepared, both parallel and perpendicular to the grooves. For the precise measurement of surface displacement, coordinate measuring machine (CMM) was used. Due to the large number of points that need to be measured, an appropriate program was supplied for the device to measure all the points automatically. In this regard, MATLAB software was used for programming, then the written program was copied into the command section of the software, and the software was then run. The specimen was divided into 48 points of measurement longitudinally and 20 points along the thickness (3mm) which totally made 1029 point. Another important point is that, it is necessary to measure both cross sections in one direction, and in fact the point of origin is identical and corresponds precisely to the front point. The piece is also completely symmetrical, relative to the cutting plane. The measured surface data has some noise as a result of measurement errors and surface roughness. The noises should, therefore, be eliminated while the overall surface shape is preserved. The coordinates of the measured points were entered into the MATLAB software, and then, using the cftool command, the MATLAB software obtained the surface curve equation. Fig. 4 shows the curved image obtained from the MATLAB software.

Obtained surface curve from MATLAB software should be placed in FEM simulation of the Contour method as the displacement of the workpiece.

3. Results and Discussion

Contour method evaluates the residual stresses by measuring deformation caused by the release of residual stresses after the precise cut of the sample. In this study, the measured displacement information was used in finite element modeling and the analysis of samples, using ABAQUS software to calculate residual stress. The inverse of smoothed data has been entered as the boundary conditions of displacement for the FEM modeling. In the next step, two-dimensional contour maps of the residual stresses were measured perpendicular to the measuring surface. The residual stresses in the defined paths were then compared. Fig. 5 shows two-dimensional contour map of residual stresses obtained from 1 pass CGPed sample on the cutting surface perpendicular to the grooves.

Also Fig. 6 shows the two-dimensional contour map of residual stresses obtained from CGP processes for the first pass, on the cutting surface parallel to the grooves.

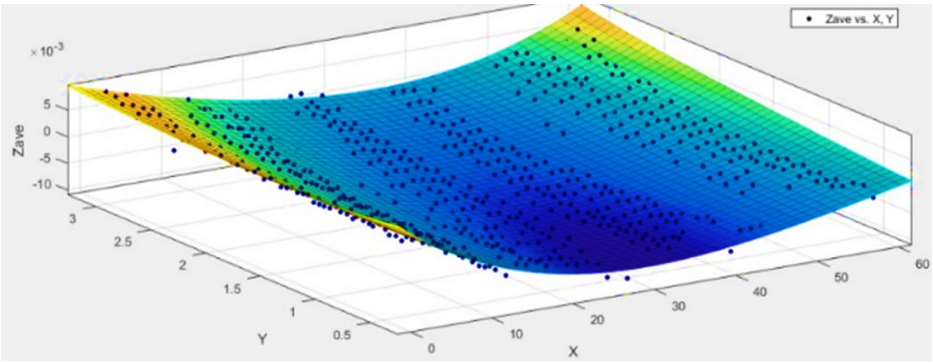

Fig. 4. The obtained contour from MATLAB software.

Fig. 5. Two-dimensional contour of residual stress on the cutting surface perpendicular to the grooves for CGP process obtained from ABAQUS software (1st pass of CGP as a sample).

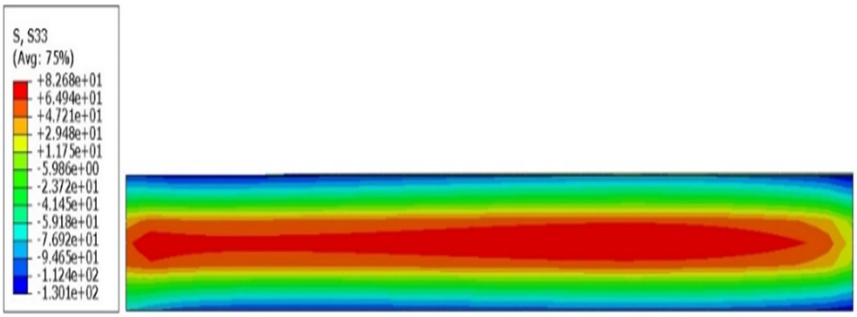

Fig. 6. Two-dimensional contour of residual stress on the cutting surface parallel to the grooves for CGP process obtained from ABAQUS software (1st pass of CGP as a sample).

To compare the results, different sections in the same paths must be examined. Therefore, to study the surfaces perpendicular and parallel to the grooves, three paths were selected on these surfaces. These paths include:
path 1: The horizontal line in the longitudinal direction in the middle of the sheet thickness.
Path 2: The vertical line along the thickness at a distance of L/3 (of length) from the center of the measurement coordinate.
Path 3: The vertical line along the thickness at a distance of 2L/3 (of length) from the center of the measurement coordinate.

Fig. 7a shows the measured residual stresses along path 1 in one and two passed CGP and UCGP states. As shown in this figure, the residual stresses are tensile along the specified path. Due to the absence of a groove at a distance of 10mm on each side of the mold, the stress values at these intervals have been close to zero and they were eliminated to focus more on the values of the graph. According to the diagram, by comparing CGPed samples with UCGPed, it can be seen that ultrasonic vibrations have reduced tensile residual stresses in the middle of the sheet thickness about 20MPa. The reduction of residual stress when applying ultrasonic vibrations has led to the use of ultrasonic stress relieving methods. Figs. 7b and 7c show the residual stress perpendicular to the surface in the thickness path. The stresses are compressive on the sheet edges and tensile in the middle of the sheet thickness. This represents that the residual stresses are self-balancing. As shown in the diagrams, the tensile residual stress in UCGP mode has significantly (about 20MPa) reduced compared to CGP mode. This reduction was also observed in the second pass. Moreover, the reduction of compressive stress on the edges of the

sheet in UCGP mode was observed compared to the CGP state.

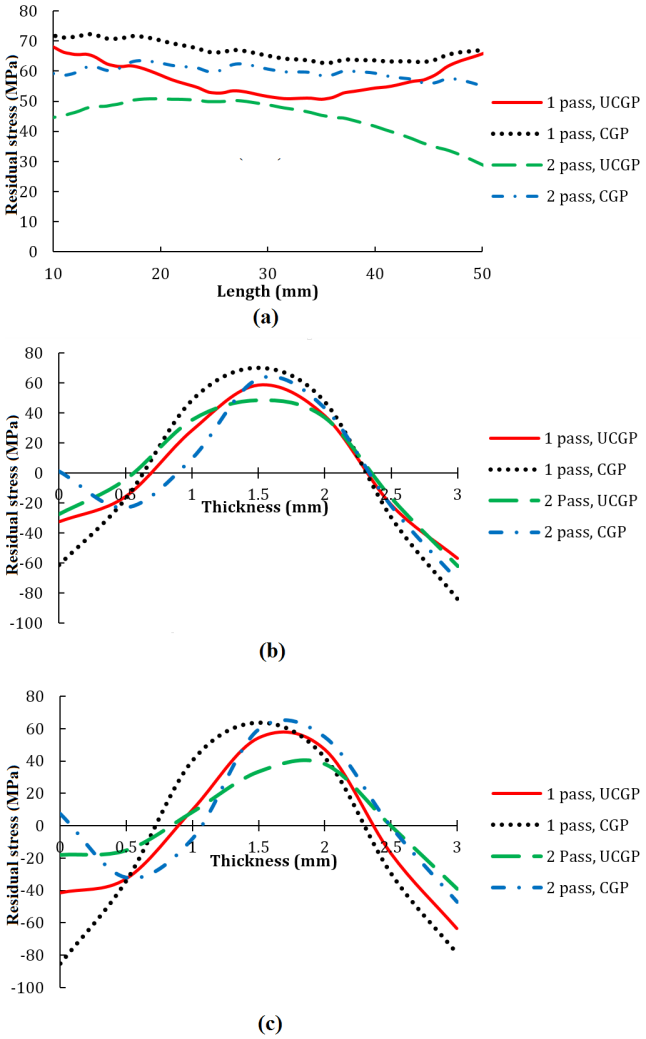

Fig. 7. Residual stress diagram perpendicular to the surface of a) Path 1, b) Path 2, c) Path 3.

Fig. 8a shows the diagram of residual stress distribution, perpendicular to the surface along the longitudinal path in the middle of the thickness of the parts. The figure indicates that using ultrasonic vibrations reduces the residual stresses significantly by 20MPa. As it can be seen in the figures, the residual stress in the middle of the sheet thickness is still tensile. Figs. 8b and 8c show a reduction in tensile residual stress in UCGP compared to CGP process in the first and second pass.

Tensile stress had a greater reduction in UCGP than CGP process in the second pass. It can also be seen that the reduction of the compressive stress on the edges of the UCGP process is more than the CGP process.

The findings show that ultrasonic vibrations usage is an effective method to decrease residual stresses which is compatible with the result of Alinaghian et al.'s study [40]. The results also showed that high-frequency vibrations can reduce the maximum tensile residual stress by 45% and increase tensile strength significantly. In another study, they also indicated that BMUAFSW can decrease the maximum longitudinal residual stress by up to 24% compared with the conventional FSW [41].

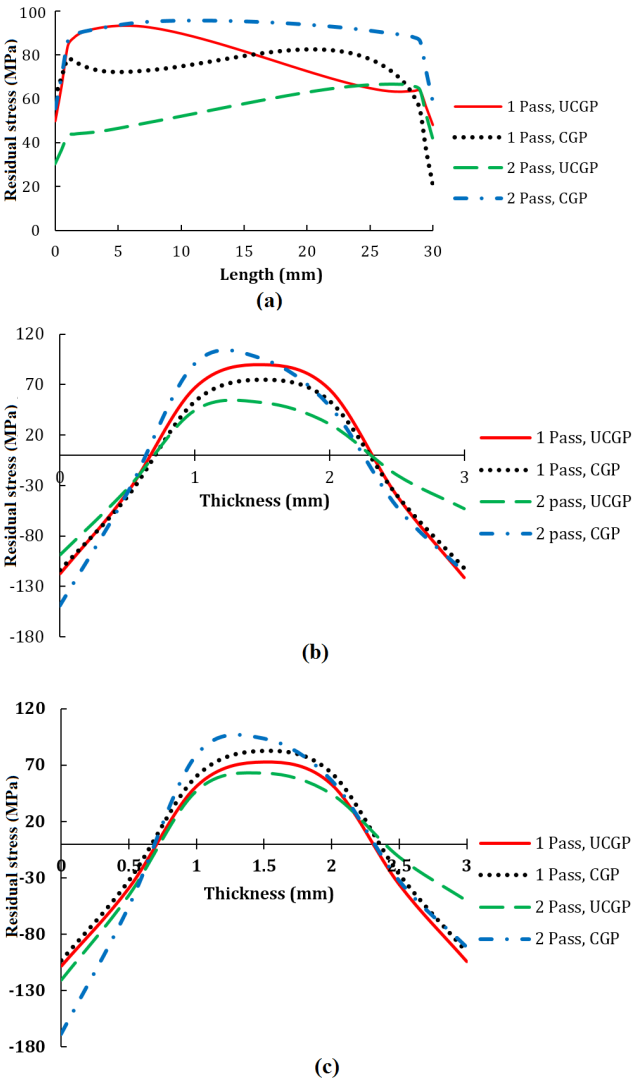

Fig. 8. Residual stress diagram perpendicular to the surface of a) Path 1, b) Path 2, c) Path 3.

4. Conclusions

In this study, the ultrasonic-assisted CGP (UCGP) process was investigated and the effects of process on the residual stress were studied by the contour method. The results showed that the stresses are compressive in the sheet edges and tensile in the middle of the sheet thickness. Also, a reduction in tensile residual stress in UCGP compared to CGP process was seen in the first and second pass.

In both UCGP and CGP and for both passes, residual stress decreased by about 20MPa while using ultrasonic vibrations compared to traditional CGP method.

References

[1] D.H. Shin, J.J. Park, Y.S. Kim, K.T. Park, Constrained groove pressing and its application to grain refinement of aluminum, Mater. Sci. Eng. A, 328(1-2) (2002) 98-103.

[2] A. Krishnaiah, U. Chakkingal, P. Venugopal, Production of ultrafine grain sizes in aluminium sheets by severe plastic deformation using the technique of groove pressing, Scr. Mater., 52(12) (2005) 1229-1233.

[3] J.W. Lee, J.J. Park, Numerical and experimental investigations of constrained groove pressing and rolling for grain refinement, J. Mater. Process. Technol., 130-131 (2002) 208-213.

[4] J. Alkorta, J.G. Sevillano, Nanomaterials by Severe Plastic Deformation: NANOSPD2, (2002) 491-497.

[5] E. Rafizadeh, A. Mani, M. Kazeminezhad, The effects of intermediate and post-annealing phenomena on the mechanical properties and microstructure of constrained groove pressed copper sheet, Mater. Sci. Eng. A, 515(1-2) (2009) 162-168.

[6] D.H. Shin, K.T. Park, Ultrafine grained steels processed by equal channel angular pressing, Mater. Sci. Eng. A, 410-411 (2005) 299-302.

[7] F. Khodabakhshi, M. Abbaszadeh, S.R. Mohebpour, H. Eskandari, 3D finite element analysis and experimental validation of constrained groove pressing–cross route as an SPD process for sheet form metals, Int. J. Adv. Manuf. Technol., 73(9) (2014) 1291-305.

[8] E. Hosseini, M. Kazeminezhad, Nanostructure and mechanical properties of 0–7 strained aluminum by CGP: XRD, TEM and tensile test, Mater. Sci. Eng. A, 526(1-2) (2009) 219-224.

[9] F. Khodabakhshi, M. Kazeminezhad, A.H. Kokabi, Constrained groove pressing of low carbon steel: Nano-structure and mechanical properties, Mater. Sci. Eng. A, 527(16-17) (2010) 4043-4049.

[10] M. Kazeminezhad, E. Hosseini, Optimum groove pressing die design to achieve desirable severely plastic deformed sheets, Mater. Des., 31(1) (2010) 94-103.

[11] S.C. Yoon, A. Krishnaiah, U. Chakkingal, H.S. Kim, Severe plastic deformation and strain localization in groove pressing, Comput. Mater. Sci., 43(4) (2008) 641-645.

[12] F. Roters, D. Raabe, G. Gottstein, Work hardening in heterogeneous alloys-a microstructural approach based on three internal state variables, Acta Mater., 48(17) (2000) 4181-4189.

[13] A. Shirdel, A. Khajeh, M.M. Moshksar, Experimental and finite element investigation of semi-constrained groove ressing process, Mater. Des., 31(2) (2010) 946-950.

[14] A. Krishnaiah, U. Chakkingal, P. Venugopal, Applicability of the groove pressing technique for grain refinement in commercial purity copper, Mater. Sci. Eng. A, 410-411 (2005) 337-340.

[15] A. Takayama, X. Yang, H. Miura, T. Sakai, Continuous static recrystallization in ultrafine-grained copper processed by multi-directional forging, Mater. Sci. Eng. A, 478(1-2) (2008) 221-228.

[16] Y. Estrin, H. Mecking, A unified phenomenological description of work hardening and creep based on one-parameter models, Acta Mater., 32(1) (1984) 57-70.

[17] Y. Estrin, L.S. Tóth, A. Molinari, Y. Bréchetc, A dislocation-based model for all hardeningstages in large strain deformation, Acta Mater., 46(15) (1998) 5509-5522.

[18] F. Nazari, M. Honarpisheh, Analytical model to estimate force of constrained groove pressing process, J. Manuf. Processes, 32 (2018) 11-19.

[19] F. Nazari, M. Honarpisheh, Analytical and experimental investigation of deformation in constrained groove pressing process, Proceedings of the Institution of Mechanical Engineers, J. Mech. Eng. Sci., 233(11) (2019) 3751-3759.

[20] F. Nazari, M. Honarpisheh, H. Zhao, Effect of stress relief annealing on microstructure, mechanical properties, and residual stress of a copper sheet in the constrained groove pressing process, Int. J. Adv. Manuf. Technol., 102(9-12) (2019) 4361-4370.

[21] M. Lucas, Vibration sensitivity in the design of ultrasonic forming dies, Ultrasonic, 34(1) (1996) 35-41.

[22] G.S. Schajer, Measurement of non-uniform residual stresses using the hole-drilling method, Part I-Stress calculation procedures, J. Eng. Mater. Technol., 110(4) (1988) 338-343.

[23] M. Sedighi, M. Honarpisheh, Experimental study of through-depth residual stress in explosive welded Al-Cu-Al multilayer, Mater. Des., 37 (2012) 577-581.

[24] M. Sedighi, M. Honarpisheh, Investigation of cold rolling influence on near surface residual stress distribution in explosive welded multilayer, Strength Mater., 44(6) (2012) 693-698.

[25] M.A. Moazam, M. Honarpisheh, Ring-core integral method to measurement residual stress distribution of Al-7075 alloy processed by cyclic close die forging, Mater. Res. Express, 6(8) (2019) 0865j3.

[26] M.A. Moazam, M. Honarpisheh, Presentation of calibration coefficient to measure Non-uniform residual stresses by the integral ring-core method, J. Stress Anal., 3(2) (2019) 15-28.

[27] M. Honarpisheh, E. Haghighat, M. Kotobi, Investigation of residual stress and mechanical properties of equal channel angular rolled St12 strips, Proceedings of the Institution of Mechanical Engineers, J. Mater. Des. Appl., 232(10) (2018) 841-851.

[28] M. Kotobi, M. Honarpisheh, Experimental and numerical investigation of through-thickness residual stress of laser-bent Ti samples, J. Strain Anal. Eng. Des., 52(6) (2017) 347-355.

[29] M. Kotobi, H. Mansouri, M. Honarpisheh, Investigation of laser bending parameters on the residual stress and bending angle of St-Ti bimetal using FEM and neural network, Opt. Laser Technol., 116 (2019) 265-275.

[30] H. Jafari, H. Mansouri, M. Honarpisheh, Investigation of residual stress distribution of dissimilar Al-7075-T6 and Al-6061-T6 in the friction stir welding process strengthened with SiO_2 nanoparticles, J. Manuf. Processes, 43(Part A) (2019) 145-153.

[31] M.A. Moazam, M. Honarpisheh, Residual stress formation and distribution due to precipitation hardening and stress relieving of AA7075, Mater. Res. Express, 6(12) (2019) 126108.

[32] M. Honarpisheh, H. Khanlari, A numerical study on the residual stress measurement accuracy using inverse eigenstrain method, J. Stress Anal., 2(2) (2018) 1-10.

[33] F. Nazari, M. Honarpisheh, H. Zhao, The effect of microstructure parameters on the residual stresses in the ultrafine-grained sheets, Micron, 132 (2020) 102843.

[34] M.B. Prime, A.R. Gonzales, The Contour Method: Simple 2D Mapping of Residual Stresses, In 6th International Conference on Residual Stresses, in Sixth International Conference on Residual Stresses, Oxford, UK, (2000).

[35] G. Johnson, Residual stress measurements using the contour method, Ph.D. Dissertation, UK: University of Manchester, (2008).

[36] D.H. Stuart, M.R. Hill, J.C. Newman Jr., Correlation of one-dimensional fatigue crack growth at cold-expanded holes using linear fracture mechanics and superposition, Eng. Fract. Mech., 78(7) (2011) 1389-1406.

[37] A. Evans, G. Johnson, A. King, P.J. Withers, Characterization of laser peening residual stresses in Al 7075 by synchrotron diffraction and the contour method, J. Neutron Res., 15(2) (2007) 147-154.

[38] L. Hacini, N. Van Lê, P. Bocher, Evaluation of residual stresses induced by robotized hammer peening by the contour method, Exp. Mech., 49 (2009) 775-783.

[39] V. Richter Trummer, P.M.S.T. De Castro, The through-the-thickness measurement of residual stress in a thick welded steel compact tension specimen by the contour method, J. Strain Anal. Eng. Des., 46(4) (2011) 315-322.

[40] I. Alinaghian, M. Honarpisheh, S. Amini, The influence of bending mode ultrasonic-assisted friction stir welding of Al-6061-T6 alloy on residual stress, welding force and macrostructure, Int. J. Adv. Manuf. Technol., 95(5-8) (2018) 2757-2766.

[41] I. Alinaghian, S. Amini, M. Honarpisheh, Residual stress, tensile strength, and macrostructure investigations on ultrasonic assisted friction stir welding of AA 6061-T6, J. Strain Anal. Eng. Des., 53(7) (2018) 494-503.

[42] M.B. Prime, A.L. Kastengren, The contour method cutting assumption: Error minimization and correction, Exp. Appl. Mech., 6 (2011) 233-250.

[43] F. Hosseinzadeh, P. Ledgard, P.J. Bouchard, Controlling the cut in contour residual stress measurements of electron beam welded Ti-6Al-4V alloy plates, Exp. Mech., 53(5) (2013) 829-839.